Electrically controlled spin-switch and evolution of Hanle spin precession in graphene

2D Materials

OPEN ACCESS

RECEIVED
9 November 2018

REVISED
27 March 2019

ACCEPTED FOR PUBLICATION
29 April 2019

PUBLISHED
13 June 2019

PAPER

Electrically controlled spin-switch and evolution of Hanle spin precession in graphene

Bing Zhao[1,2], Dmitrii Khokhriakov[2], Bogdan Karpiak[2], Anamul Md Hoque[2], Lei Xu[3], Lei Shen[3], Yuan Ping Feng[4], Xiaoguang Xu[1], Yong Jiang[1] and Saroj P Dash[2,5,6]

[1] Beijing Advanced Innovation Center for Materials Genome Engineering, School of Materials Science and Engineering, University of Science and Technology Beijing, Beijing 100083, People's Republic of China
[2] Department of Microtechnology and Nanoscience, Chalmers University of Technology, SE-41296, Göteborg, Sweden
[3] Department of Mechanical Engineering, National University of Singapore, Singapore 117575, Singapore
[4] Department of Physics, National University of Singapore, Singapore 117542, Singapore
[5] Graphene Center, Chalmers University of Technology, SE-41296 Göteborg, Sweden
[6] Author to whom any correspondence should be addressed.

E-mail: saroj.dash@chalmers.se

Keywords: spintronics, Hanle spin precession, graphene, spin injection, magnetic proximity effect

Supplementary material for this article is available online

Abstract

Next generation of spintronic devices aims to utilize the spin-polarized current injection and transport to control the magnetization dynamics in the spin logic and memory technology. However, the detailed evolution process of the frequently observed bias current-induced sign change phenomenon of the spin polarization has not been examined in details and the underlying microscopic mechanism is not well understood. Here, we report the observation of a systematic evolution of the sign change process of Hanle spin precession signal in the graphene nonlocal spintronic devices at room temperature. By tuning the interface tunnel resistances of the ferromagnetic contacts to graphene, different transformation processes of Hanle spin precession signal are probed in a controlled manner by tuning the injection bias current/voltage. Detailed analysis and first-principles calculations indicate a possible magnetic proximity and the energy dependent electronic structure of the ferromagnet-graphene interface can be responsible for the sign change process of the spin signal and open a new perspective to realize a spin-switch at very low bias-current or voltage.

Introduction

Spintronic technology requires efficient methods for the creation and utilization of spin-polarized electrons for faster and low power consumption electronics [1, 2]. Such spin current is utilized for magnetization switching governed by spin torque and spin–orbit torque phenomenon in metals-based hybrid devices without using an external magnetic field [3, 4]. However, the magnetization switching methods by spin current suffer from large power consumption due to the requirement of large current density and the involved spin-to-charge conversions processes [5]. Therefore, electronic control of spin polarization by application of a low bias voltage/current is considered desirable [1]. In this direction, the efficient creation and control of pure spin current can be the next big step for the proposed spin-based memory and logic operations [6].

Over the last few decades, various methods were discovered for electrical injection, detection and transport of spin polarization in metals [7], semiconductors [8, 9] and graphene [10] at room temperature. These comprehensive investigations involved the optimization of spin transport channel materials, ferromagnetic source and drain contacts, and tunnel barriers for efficient injection and detection of spin-polarized electrons. More often, a sign change of spin-polarization with an injection bias current/voltage has been frequently observed in a range of channel materials using different types of ferromagnetic tunnel contacts [8, 11–18]. The origin of such sign reversal is mainly ascribed to the energy-dependent spin-polarized electronic density of states (DOS) at the tunnel interface, magnetic proximity effects at the interfaces with ferromagnets, resonant tunneling and spin filtering in the tunnel barriers and interfaces [19–21].

However, the detailed measurement of the sign change transformation process of spin polarization is still lacking and its microscopic mechanism is not fully understood.

Here, we report an observation of a very systematic evolution of the sign change process of the Hanle spin precession signal by utilizing graphene spintronic devices at room temperature. To investigate this, Hanle spin signals with different injection bias currents and angles were probed in devices having different ferromagnetic tunnel contact resistances. Analysis of the results and first-principles calculations reveal that the magnetic proximity effect at the graphene-ferromagnet interfaces is responsible for the sign change process of the spin polarization. This electrically controlled sign change of spin polarization at such low currents and voltages provides a new perspective for its practical utilization as a spin-switch in memory and logic applications.

Results

The spintronic devices were nanofabricated with exfoliated few-layer graphene on SiO_2/n-Si substrates with TiO_2/Co ferromagnetic (FM) electrodes. Different devices were made with the variation of the contact resistance in the range of type-I: 0.5–1 kΩ, type-II: 1–3 kΩ, type-III: 5–10 kΩ (see Methods for details). Such variations in ferromagnetic tunnel contact parameters made it possible to investigate the continuous evaluation of sign change process of Hanle spin precession signal by controlling the injection bias current/voltage in a non-local measurement geometry (figure 1(a)). The FM contacts are used as injector, detector and reference contacts in the devices presented in the main manuscript. The devices with reference Cr/Au contacts and FM injector/detector contacts are presented in the supplementary information. The spin-valve measurements were performed at a fixed DC bias current while measuring the non-local voltage V_{nl} with an in-plane magnetic field ($B_{||}$) sweep (figure 1(b)). Hanle spin precession signals were recorded with an out-of-plane magnetic field ($B_{\perp}$) sweep while keeping Co electrodes in either a parallel (P) or anti-parallel (AP) configuration (figure 1(c)).

For very low spin-injection bias currents ($|I_{bias}| < 100$ μA), a linear response of spin signal is observed in devices as shown in figure 1(d) and supplementary figure S1(b) (stacks.iop.org/TDM/6/035042/mmedia). However, with an increase of the injection bias current, the spin signal shows strong non-linear behavior and an anomalous sign change (figure 1(d)). Figures 1(b) and (c) show measurements of such a sign inversion of the spin-valve and Hanle signals respectively at a larger bias current in a type-I device. Hanle measurements in figure 1(c) were performed for parallel orientation of ferromagnetic electrodes. The Hanle measurements for anti-parallel configuration of ferromagnet also showed similar sign change behavior with bias current as presented in supplementary figure S1(a).

Figure 1(d) shows the spin-valve signal amplitude ΔV_{nl} as a function of injection bias current for a type-I device. For the positive bias current, corresponding to the spin extraction regime, a strong non-linear spin signal and a sign change is reproducibly observed. However, no sign inversion is observed for the negative bias currents corresponding to the spin injection regime. The spin signal amplitude with corresponding bias voltage across the injector junction for type-I, -II and -III devices with different interface resistances are plotted in Supplementary information figure S1(c). To demonstrate that such a sign change behavior can be used as a spin-switch device, a square wave shape current was applied to the injector electrode in Device 2 (type-II). As expected, a two-state switching of the spin signal was observed (figure 1(e)), which offers a practical method to use the low current-induced switching of the spin signal. The switching current density is usually in the range 10^7–10^9 A m^{-2} corresponding to the transition point 5–500 μA of our devices depending on the resistance of the ferromagnetic tunnel contacts.

Although such sign change of the spin signal has been reported previously in different spin transport devices, the detailed evolution of sign change process of the spin polarization at the transition bias current/voltage region has never been detected experimentally. In order to investigate the detailed sign change process in the transition region, Hanle spin precession measurements were performed as shown in figure 2(a) for a type-I device. Surprisingly, we observed drastically different Hanle line shapes at these transition bias current (between $I_{bias} = 300$–400 μA), which are in contrast to the standard spin precession signals [10]. In these transient Hanle data, a dip appears at zero magnetic field and grows until the complete sign change occurs in the Hanle curve.

To phenomenologically extract the magnitudes of the competing mechanisms, a simple model is adopted (see details in Note1). From the data fitting, we roughly extract the magnitude for both components of Hanle spin signals as shown in figure 2(c). While one component of the spin signal increases with injection bias current, the other decreases. We notice the different half-line widths between the two Hanle curves of opposite sign, like for $I = 200$ μA and 500 μA in figure 2(a). According to the previous studies, not only the spin lifetime of the graphene, but also contact resistance, graphene channel length, spin diffusion constant, and DC bias induced drift and thermal effects can affect the half-line width of the measured Hanle curve. Here, considering the fact that all the Hanle curves were obtained from the same device, we can rule out all factors mentioned above in our experiment except the DC bias related effects. Considering these multiple bias related drift, diffusion and thermal effects, the exact estimation of spin lifetime from these Hanle curves are not possible, as a proper model and

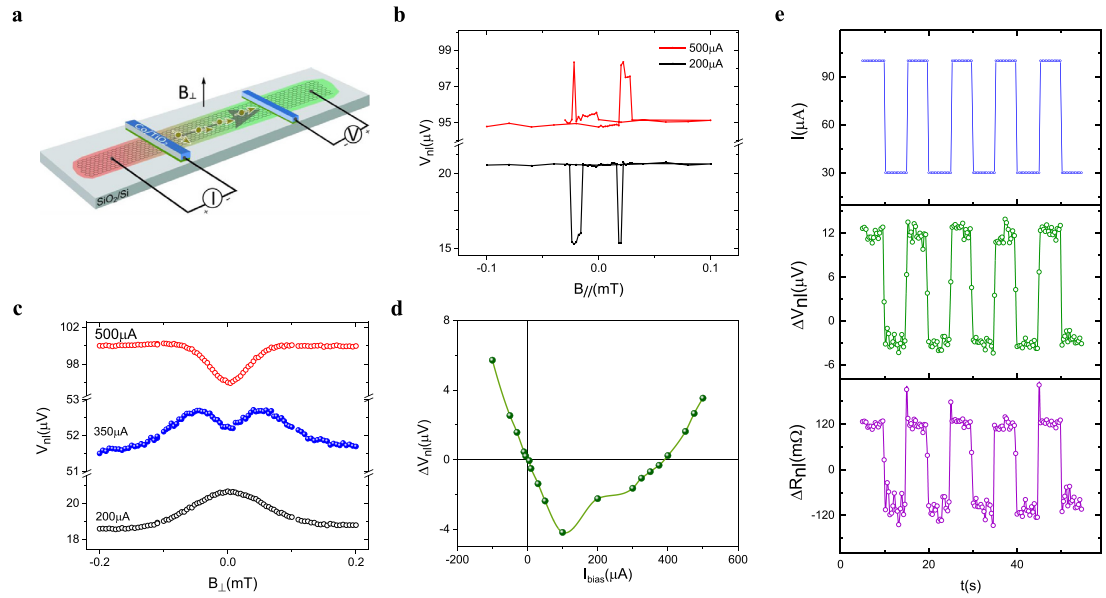

Figure 1. Sign change of spin signal and spin-switch operation in a graphene device at room temperature. (a) Schematic of the graphene spintronic device with ferromagnetic tunnel contacts (TiO_2/Co) in a non-local measurement configuration. (b) and (c) Nonlocal spin-valve and Hanle signals measured with different DC bias currents in the non-linear regime showing a sign change for Dev 1. Hanle measurements were performed for parallel orientation of ferromagnetic electrodes. Here we used a type-I device with contact resistance is ~0.5–1 kΩ. (d) The measured spin-valve signal magnitude $\Delta V_{nl} = V_{nl}(AP) - V_{nl}(P)$ for Dev-1 as a function of bias current, showing non-linear behavior and an anomalous sign change at a larger positive bias current range. (e) A spin-switch signal of the Dev-2 with an application of a square wave shape injection current (at $I_{bias} = 30\ \mu$A and 100 μA), due to sign change of the spin signal. The plots show—upper panel: the applied current wave, middle panel: measured ΔV_{nl} and the lower panel: $\Delta R_{nl} = \Delta V_{nl}/I$.

understanding of the transition Hanle curves is still lacking. To be noted, for devices with higher contact resistances of type-II and III, the sign change behavior is also observed. However, no Hanle signal is observed at the transition bias points within the measurement noise level (see supplementary figures S1(c) and S2). The transition bias current for the sign change is found to decreases with increasing contact resistance. We would like to note that one can also expect the continuous evolution of Hanle signal and its anomalous behavior with bias current where the ferromagnetic contacts are also used as a reference electrode in the non-local injector circuit. However, the sign change phenomenon of the spin signal is present even with the devices with nonmagnetic Cr/Au reference contacts. For a detailed discussion see supplementary note 4.

To further examine the behavior of the spins injected at the transition states, angle dependent measurements of the Hanle effect were performed at different magnetic field orientation at a constant injection bias current (figure 3(a)). A clear decrease of the Hanle signals at the transition bias current was observed when the B field approached to lower angles, because no more precession is expected when B field is aligned with injected spins (figure 3(b)). These measurements indicate that spin orientations at the transition stage are in the graphene plane. The angle dependence of the spin precession signal at different bias currents before and after the transition bias current are shown in figures 3(c) and (d). As expected, the Hanle signals disappear when the spins and B field are in the same orientation. Analysis of anisotropic spin relaxation in graphene for the Hanle curves at different bias currents gives $\xi \sim 1$ (figure 3(e) and see details in supplementary note 2). This implies that the transition Hanle curve is not due to an anisotropy [22–24] of the spin lifetime in the graphene channel.

We also performed control experiments to understand the origin of the sign change process of the spin signals. The bias current-induced spin drift effect [25, 26] should be considered, as it can also enhance or suppress the spin signal magnitude depending on the spin injection or extraction process giving rise to an asymmetric bias-dependent behavior. Although, the non-linear behavior of the spin polarization with a bias current has been observed due to electric field drift contribution to the spin accumulation, the sign change of the signal due to drift is not expected [25, 26]. Secondly, thermal effects due to large bias current should be taken into consideration, such as thermal spin injection at the injector [27] and thermoelectric spin voltage [28] in the channel, which can also contribute to enhancement and suppression of spin signal and can also cause sign inversion of the spin signal. In the supplementary figures S3 and S4, control experiments are shown for heating of graphene channel and also the ferromagnetic electrode (see details in Supplementary Note 3 and Note 4). We observe neither any noticeable change in the magnitude of the spin signal nor any change of their sign with heating of the graphene channel and ferromagnetic contacts within the measurement noise for these DC bias experiments. These results are consistent with negligible thermal

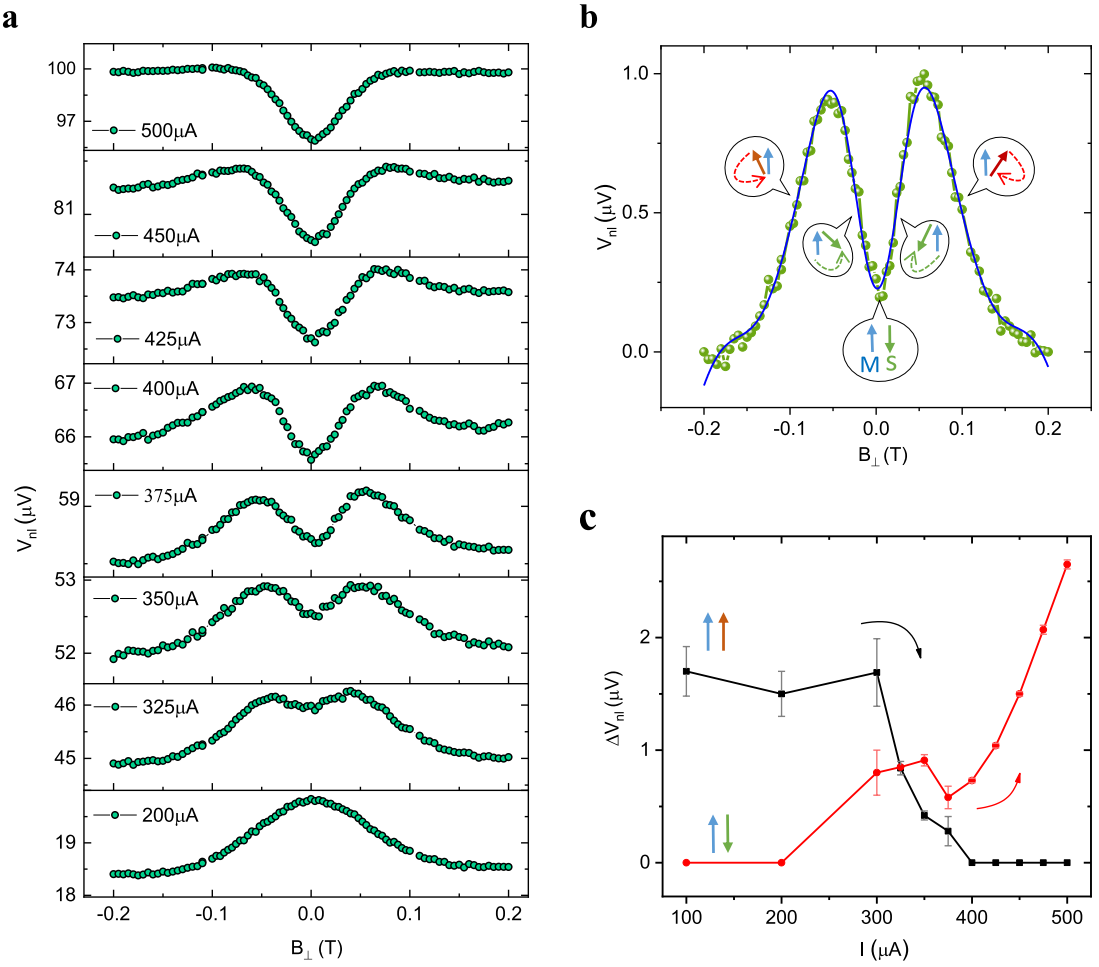

Figure 2. Hanle spin precession signal during spin reorientation process for a type-I device. (a) Evolution of the measured Hanle spin precession sign change behavior with an injection bias current of 200–500 μA at room temperature. (b) The transient Hanle curve at $I_{bias} = 375$ μA is fitted by a model considering two Hanle curves of opposite signs using equation S(1) in supplementary note 1. The blue arrows represent the detector magnetization direction and the spin orientations in green and red color with opposite directions. A linear background is removed from the Hanle curve. (c) The magnitude of the two components of the spin signal with bias current as obtained from Hanle fitting.

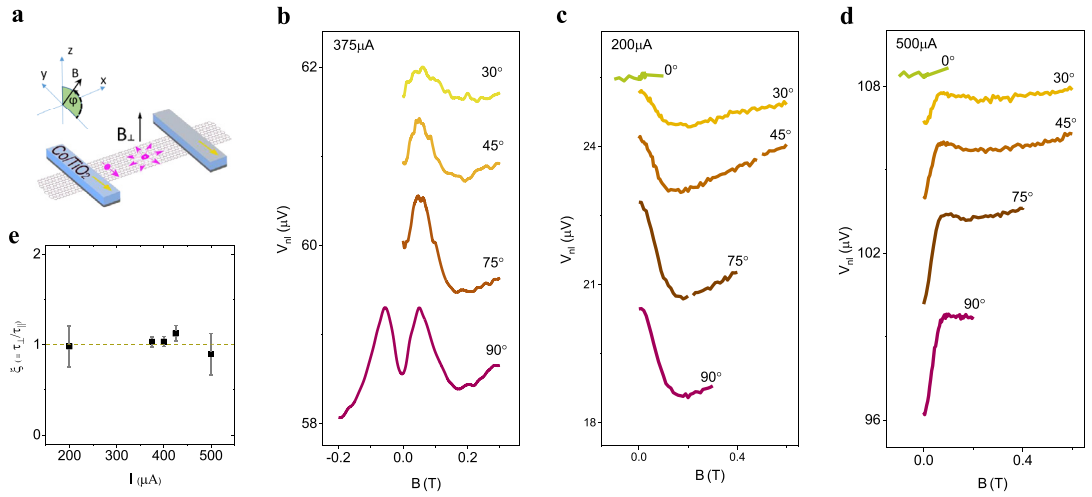

Figure 3. Angle dependence of the Hanle curves at different bias currents. (a) The schematics of the measurement geometry with different angles of the external magnetic field (B) with respect to the magnetization of the ferromagnet. (b)–(d) Angle dependence of the Hanle curves of Type-I device at bias currents of 375 μA, 200 μA, and 500 μA, respectively. (e) Spin relaxation anisotropy time $\xi = \tau_{\perp}/\tau_{//}$, where $\tau_{//}$ and $\tau_{\perp}$ are the lifetime for the in-plane and perpendicular spins. The ξ is plotted for the Hanle data at different injection bias currents.

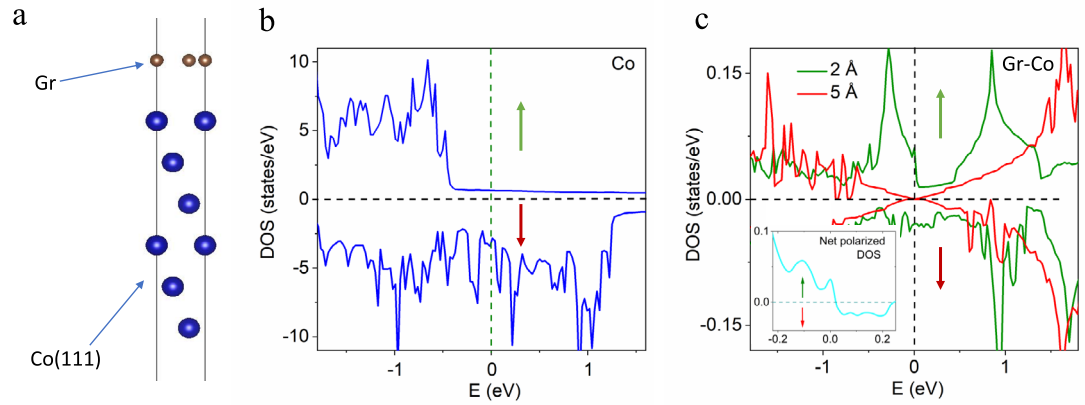

Figure 4. The first-principles calculation of proximity effect induced sign reverse of polarization. (a) The model is consist of graphene and six layers of Co (1 1 1). (b) The DOS of up and down spins in Co. (c) The DOS of up and down spins in graphene with the graphene-Cobalt interface distance of 2 Å and 5 Å. The inset is a net polarized DOS with the 2 Å case.

effect expected for our highly doped graphene samples [28]. To be noted, both the thermal control experiments and standard spin transport measurements were performed by the same DC current measurement technique. However, the local hot-electron effects across the tunnel contacts are expected to be present in such large DC injection bias currents. Considering the nonlocal measurement geometry, the magnitude and the bias dependence of the signal, we can also rule out the effect of magnetoresistance due to impurity states in the barrier [29] as the origin of the sign change and Hanle precession transitions. Moreover, the origin from the stray field induced extra spin precession can also be ruled out as it should be present at all the bias current measurements instead of only at the transition point [30].

For a better understanding of the sign change process of the spin signal, we also performed a first-principles calculation [31–33]. The model is constructed by considering a graphene layer and six layers of Co (1 1 1) (figure 4(a)). The lattice constant of the heterostructure is set to the experimental value of Co [34] with lattice mismatch around 1.5%. The optimized interface distance between graphene and Co is estimated to be ~2 Å. Here, we set interface distance to 2 Å and 5 Å to calculate the distance dependence of the magnetic proximity effect of Co on graphene. When the interface distance is large (5 Å), the states of graphene around Fermi level are unpolarized and the Dirac cone is well preserved (figure 4(c)). Due to the strong proximity effect at a shorter interface distance of 2 Å, the up spins became the majority, different from the ones in Co (figure 4(b)). As a result, when graphene and Co are close enough (like pinhole area through thin TiO_2 tunnel barrier), the spin polarization for electrons from Co electrode and graphene-Co hybrid interface can be opposite to each other. Spin polarization at the interface is directly related to the DOS of Co and graphene-Co hybrid interface. As shown in figure 4(b), the DOS of Co is quite stable in an energy window of about 700 meV below the Fermi level [35]. However, the DOS of graphene-Co hybrid interface around Fermi level is strongly energy dependent (figure 4(c)). As shown in the inset of figure 4(c), a small shift of the position of the Fermi level can tune the relative dominance of the up and down spins. Therefore, a small bias current/voltage or gate voltage at the hybrid interface can induce a sign reversal of spin polarization [15].

If magnetic proximity effect at the graphene/Co interface is the underlying physical mechanism in our experiments, one would expect that the sign reversal and abnormal Hanle curves will not be observed for thicker TiO_2 tunnel barriers at the interface. To be noted, for devices with thicker TiO_2 having higher contact resistances (type-II and III devices), the complete sign change behavior is also observed. However, no anomalous Hanle signal is observed at the transition bias points within the measurement noise level (see supplementary figures S1(c) and S2). Moreover, a similar sign change behavior using different barrier materials have been observed [13, 17, 36]. However, such systematic change of sign via an anomalous Hanle signal at the transition points has not been reported before. These previous work also involves the use of atomically flat h-BN tunnel barrier (1–3 layers, up to 1.2 nm thick), where a sign change is also reproducibly observed [13, 17, 36]. As the theory papers predict, the magnetic proximity effect can extend across a tunnel barrier [37, 38]. However, if the barrier is too thick, we run into a practical problem, i.e. we usually cannot observe nonlocal spin signal anymore because of very high contact resistances. By comparing experiments with the theoretical calculations, we can conclude that the magnetic proximity effect at the Co-graphene hybrid interfaces and its highly energy dependent electronic structure can be one of the mechanisms of the observed sign change behavior of spin polarization and anomalous Hanle behavior.

Summary

In summary, we reported the evolution of the sign inversion process of the spin signal in the graphene

nonlocal spin devices with an anomalous behavior by probing the transition phases of Hanle curves in a systematic manner. The anomalous Hanle curves with "dip features" at the transition bias currents can be explained by considering either magnetic proximity effect or the contribution from the reference ferromagnetic electrodes in the injector circuit. However, the sign change process of the spin signal is universal and is also present in the devices with non-magnetic reference electrodes. Although, the controlled heating of the FM and graphene did not lead to any observable sign change behavior in the DC measurements, the local hot-electron effects across the tunnel contacts are expected to be present in such large DC injection bias currents. Further understanding and accurate modeling is required to explain the observed anomalous Hanle curves. Considering our experiments and theoretical calculations, the magnetic proximity effect and energy-dependent complex electronic structure of the ferromagnet-graphene hybrid interfaces are believed to be one of the possible reason for the sign change of the spin polarization. The controlled change of spin polarization direction at a very low voltage and currents does not only help us to understand the basic spin injection mechanism but also offers a new perspective to utilize the spin-switch functionality. Utilization of such electronic control of spin phenomena may pave the way to realize the novel graphene-based spintronic devices with low power consumption.

Methods

The few-layer graphene were mechanically exfoliated from HOPG onto the n-doped Si substrate with 300 nm SiO_2. To obtain different contact resistance, three recipes were used during the preparation of the tunnel barrier. Type-I: A one step deposition and oxidation process: 0.6 nm Ti was deposited at 8° from the normal incidence angle followed by a 30 Torr O_2 oxidation for 2 h. Type-II: A one-step deposition and oxidation process: 1 nm Ti was deposited at 90° followed by a 20 Torr O_2 oxidation for 2 h. Type-III: A two-step deposition and oxidation process, 0.5 nm Ti was deposited at 8° followed by a 30 Torr O_2 oxidation for 1 h and again 0.6 nm Ti was deposited at 8° followed by a 30 Torr O_2 oxidation for 2 h. All the recipes are followed by a 60 nm Co deposition. These recipes offer us three different contact resistance in the range Type-I: 0.5–1 kΩ, Type-II: 1–3 kΩ and Type-III: 5–10 kΩ, which make it possible to systematically study the sign inversion of nonlocal Hanle spin signal. Moreover, rotation of the chip during titanium deposition were used for all the three recipes. No annealing was used to avoid degeneration of the ferromagnetic contacts. All the measurements are performed in a cryostat under vacuum at room temperature using a current source Keithley 6221, a nanovoltmeter Keithley 2182A.

Acknowledgments

Additional information

The authors at Chalmers University of Technology, Sweden acknowledge financial supports from EU Graphene Flagship (GrapheneCore2 contract number 785219), EU FlagEra project (from Swedish Research council VR No. 2015-06813), Swedish Research Council VR project grants (No. 2016-03658), Graphene center and the AoA Nano program at Chalmers University of Technology. The authors from University of Science and Technology Beijing, China, acknowledge financial supports from the National Basic Research Program of China (Grant No. 2015CB921502) and the National Natural Science Foundation of China (Grant Nos. 51731003, 51471029). Bing Zhao would like to thank the financial support from the program of China Scholarships Council (File No. 201706460036). The authors at National University of Singapore acknowledge financial supports from R-256-000-615-114, MOE, Singapore.

Contributions

BZ, DK, BK, SPD fabricated and measured the devices at Chalmers University of Technology. BZ and SPD analyzed, interpreted the experimental data, compiled the figures and wrote the manuscript. LX, LS, XX and YPF performed the first principles calculation. DK, BK, AMH, XX, YJ discussed the results and provided feedback on the manuscript. SPD, YJ and YPF supervised the experimental and theoretical research. SPD conceived the idea and supervised the project.

Competing interests

The authors declare no competing financial interests.

Data availability

The data that support the findings of this study are available from the corresponding authors on reasonable request.

ORCID iDs

Bing Zhao https://orcid.org/0000-0002-5560-6750
Bogdan Karpiak https://orcid.org/0000-0001-7462-8405
Xiaoguang Xu https://orcid.org/0000-0001-7659-865X
Saroj P Dash https://orcid.org/0000-0001-7931-4843

References

[1] Chappert C, Fert A and Van Dau F N 2007 *Nat. Mater.* **6** 813
[2] Behin-Aein B, Datta D, Salahuddin S and Datta S 2010 *Nat. Nanotechnol.* **5** 266
[3] Slonczewski J C 1996 *J. Magn. Magn. Mater.* **159** L1
[4] Miron I M, Garello K, Gaudin G, Zermatten P J, Costache M V, Auffret S, Bandiera S, Rodmacq B, Schuhl A and Gambardella P 2011 *Nature* **476** 189
[5] Wang M, Zhang Y, Zhao X and Zhao W 2015 *Micromachines* **6** 1023
[6] Žutić I, Fabian J and Das Sarma S 2004 *Rev. Mod. Phys.* **76** 323
[7] Jedema F J, Filip A T and Van Wees B J 2001 *Nature* **410** 345
[8] Lou X, Adelmann C, Crooker S A, Garlid E S, Zhang J, Reddy K S M, Flexner S D, Palmstrøm C J and Crowell P A 2007 *Nat. Phys.* **3** 197
[9] Dash S P, Sharma S, Patel R S, De Jong M P and Jansen R 2009 *Nature* **462** 491
[10] Tombros N, Jozsa C, Popinciuc M, Jonkman H T and van Wees B J 2007 *Nature* **448** 571
[11] Valenzuela S O, Monsma D J, Marcus C M, Narayanamurti V and Tinkham M 2005 *Phys. Rev. Lett.* **94** 196601
[12] Dankert A, Dulal R S and Dash S P 2013 *Sci. Rep.* **3** 3196
[13] Kamalakar M V, Dankert A, Kelly P J and Dash S P 2016 *Sci. Rep.* **6** 21168
[14] Gurram M, Omar S and van Wees B J 2017 *Nat. Commun.* **8** 248
[15] Ringer S, Rosenauer M, Völkl T, Kadur M, Hopperdietzel F, Weiss D and Eroms J 2018 *Appl. Phys. Lett.* **113** 132403
[16] Xu J, Singh S, Katoch J, Wu G, Zhu T, Žutić I and Kawakami R K 2018 *Nat. Commun.* **9** 2869
[17] Zhu T, Singh S, Katoch J, Wen H, Belashchenko K, Žutić I and Kawakami R K 2018 *Phys. Rev.* B **98** 054412
[18] Zhao B, Xu X, Wang L, Li J, Zhang Z, Liu P, Liu Q, Wang Z and Jiang Y 2018 *Carbon* **127** 568
[19] Lazić P, Sipahi G M, Kawakami R K and Žutić I 2014 *Phys. Rev.* B **90** 085429
[20] Wu Q, Shen L, Bai Z, Zeng M, Yang M, Huang Z and Feng Y P 2014 *Phys. Rev. Appl.* **2** 044008
[21] Yu Z G, Baker J and Krishnamurthy S 2010 *Phys. Rev.* B **82** 035425
[22] Cummings A W, Garcia J H, Fabian J and Roche S 2017 *Phys. Rev. Lett.* **119** 206601
[23] Benítez L A, Sierra J F, Savero Torres W, Arrighi A, Bonell F, Costache M V. and Valenzuela S O 2018 *Nat. Phys.* **14** 303
[24] Ghiasi T S, Ingla-Aynés J, Kaverzin A A and Van Wees B J 2017 *Nano Lett.* **17** 7528
[25] Józsa C, Popinciuc M, Tombros N, Jonkman H T and van Wees B J 2008 *Phys. Rev. Lett.* **100** 236603
[26] Ingla-Aynés J, Meijerink R J and van Wees B J 2016 *Nano Lett.* **16** 4825
[27] Slachter A, Bakker F L, Adam J-P and van Wees B J 2010 *Nat. Phys.* **6** 879
[28] Sierra J F, Neumann I, Cuppens J, Raes B, Costache M V and Valenzuela S O 2018 *Nat. Nanotechnol.* **13** 107
[29] Txoperena O, Song Y, Qing L, Gobbi M, Hueso L E, Dery H and Casanova F 2014 *Phys. Rev. Lett.* **113** 146601
[30] Dash S P, Sharma S, Le Breton J C, Peiro J, Jaffrès H, George J M, Lemaître A and Jansen R 2011 *Phys. Rev.* B **84** 054410
[31] Kresse G and Furthmüller J 1996 *Phys. Rev.* B **54** 11169
[32] Perdew J P, Burke K and Ernzerhof M 1996 *Phys. Rev. Lett.* **77** 3865
[33] Kresse G and Joubert D 1999 *Phys. Rev.* B **59** 1758
[34] Cerda J R, de Andres P L, Cebollada A, Miranda R, Navas E, Schuster P, Schneider C M and Kirschner J 1993 *J. Phys.: Condens. Matter* **5** 2055
[35] Blaha P, Schwarz K and Dederichs P H 1988 *Phys. Rev.* B **38** 9368
[36] Leutenantsmeyer J C, Ingla-Aynés J, Gurram M and van Wees B J 2018 *J. Appl. Phys.* **124** 194301
[37] Lazić P, Belashchenko K D and Žutić I 2016 *Phys. Rev.* B **93** 241401
[38] Žutić I, Matos-Abiague A, Scharf B, Dery H and Belashchenko K 2019 *Mater. Today* **22** 85